TRANSACTIONS OF THE INSTITUTE OF FLUID-FLOW MACHINERY

No. 133, 2016, 55–68

David Garcia[a*], Grzegorz Liśkiewicz[b]

Stable or not stable? Recognizing surge based on the pressure signal

[a] *Mechanical and Aerospace Engineering, University of Strathclyde, 75 Montrose Street Glasgow G1 1XJ, UK*

[b] *Institute of Turbomachinery, Lodz University of Technology, 219/223 Wólczańska, 90-924 Łódź, Poland*

Abstract

The surge protection may be worth millions of dollars. This is typical price of a centrifugal compressor repair combined with additional cost of nonfunctionality of an industry employing it. This threat is normally secured by application of an antisurge systems. Typically they are activated at predefined working conditions when compressor mass flow rate approaches region affected by the surge. As a result those systems are vastly limiting its operational range usually by a desirable region where compressor attains large pressure ratio. Therefore, a modern anti-surge systems are aiming at diminishing this tradeoff by reacting to the real pressure signal gathered at high frequency. This paper presents one of those methods employing singular spectrum analysis. This algorithm has not been widely used for this application, while it was shown herein that it may bring clear distinction between stable and nonstable working condition, even at presurge conditions. Hence in further perspective it may bring anti-surge protection quality, that was not met with another methods.

Keywords: Singular spectrum analysis; Nonlinear dynamics; Statistical pattern recognition; Compressor; Surge

*Corresponding Author. Email address: david.garcia@strath.ac.uk

1 Introduction

1.1 Unstable phenomena in centrifugal compressors

Unstable phenomena in centrifugal compressors were first identified by Emmons in 1950s [1]. In 1976 Greitzer introduced a mathematical model describing a development of surge [2], which was verified by an experiment [3]. Till now, the model was analysed and developed by numerous researchers including Hansen *et al.* [4], Elder and Gill [5], Fink *et al.* [6], Gravdahl and Egeland [7], Willems [8], Meuleman [9], Helvoirt [10] and more recently Yoon *et al.* [11]. There are also examples of another attempts of simulating surge. Macdougal and Elder [12] used relations for a polytropic compression process in combination with principles of conservation of mass, momentum and energy. This method was followed by Badus *et al.* [13] and Botros [14] including variation of the impeller speed. These three models can be applied to both axial and centrifugal compression systems, nevertheless, they are quite complex.

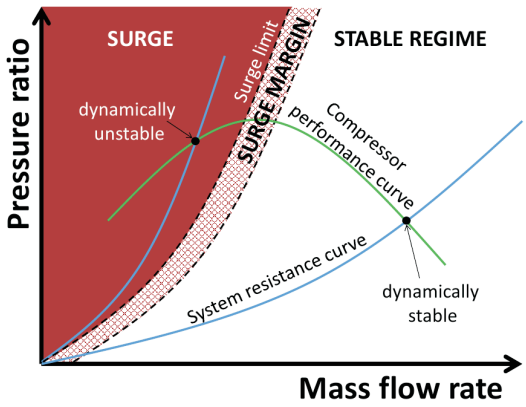

Figure 1: Compressor performance curve, system resistance curve and the surge region.

In above mentioned works a concept of surge limit was introduced. Figure 1 shows a performance curve of a compressor. Area on the left side of the surge limit is beyond the capabilities of the device due to the fact that there is a high risk of unstable work conditions appearance. On the other hand, the compressor operating in the vicinity of the surge limit achieves the highest pressure ratio and high efficiency. Therefore, this is a very attractive region from the point of view of the user. That is why a surge phenomenon, as well as local unstable structures

(rotating stall [15–16] and inlet recirculation [17]) remain a subject of interest for a wide range of scientists trying to develop modern antisurge devices [18].

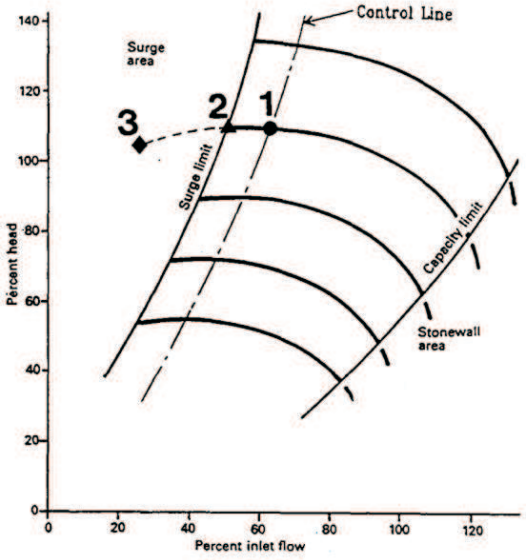

Figure 2: Classification of anti-surge systems by their moment of reaction: 1 – prevention, 2 – fast detection, 3 – active control [18].

Figure 2 shows a classification of antisurge control systems by their moment of activation. The simplest ones (no. 1) reduce the compressor operational range to a certain region, which is separated from the surge limit by a predefined surge margin. This is the cheapest solution, yet, not always effective and limiting the system operational range. Another class of antisurge systems is based on a rapid instability detection (no. 2). Their effectiveness depends on the algorithm applied. Active antisurge control units are also considered (no. 3), where the oscillations are damped enabling the compressor to safely operate in a region which is potentially subjected to a surge phenomenon. The biggest disadvantages of the solutions no. 2 and no. 3 include their operational costs and at the same time their lack of versatility. That is why, researchers constantly seek a better design in the field of antisurge control units, which would reconcile two diverging aims – guarantee of safety and operation in close vicinity of the surge.

Figure 2 visualizes the fact of high potential of an active antisurge systems. Therefore it is not surprising that many researchers examined this type of surge protection schemes. It could be generalized that any protection system of that type is based on an input signal and uses a controller that steers some adjustable

elements. In most cases it was an adjustable valve [19–22], while Williams and Huang [23] and Jungowski *et al.* [10] considered speaker, Gysling *et al.* [7] moving wall in plenum, and Gravadhl *et al.* [13] variable shaft speed. Regardless of the chosen solution, there are some common problems of the active antisurge systems. This includes mainly a large level of complexity, high operational costs as well as lack of 100% guarantee of their reliability.

Antisurge systems based on the detection of the phenomena prior to surge are free from those problems and still provide operation in close vicinity of the surge margin. Those systems react on first surge indicators such as the mass flow decrease [24] or local flow separation [25]. It could be also based on simple pressure measurement subject to specific algorithm. One of them is singular spectrum analysis (SSA) which is an extension of principal component analysis (PCA) for nonindependent signals [26,27]. The SSA method allows to limit the signal analysis to a few first components that possess the greatest impact on the result. The method is widely used for the signal compression, trends prediction, structural damage detection [28]. The number of attempts to apply this method to surge detection is limited, yet provided promising conclusions [29,30].

Results of [31] have shown that after implementing SSA the compressing system had limited dimension and could be represented with just a few first principal components. Usually using three is enough because they contain the majority of the variance in the principal components decomposition. Moreover, it was shown that the first principal component was reproducing the value of the average pressure. Most promising for surge detection were components number two and three. In two dimensional space constructed from them the phase portrait of a signal changed into limit cycle with strong oscillations at inception of unstable flow structures. Moreover, this method has proven to be sensitive to all kinds of flow instabilities: local (like inlet recirculation) or global (like surge).

The aim of this paper is to continue this effort and analyze the effect of clustering of signals subject to SSA. In other words clustering appears when points from stable and unstable operation group in different spaces after SSA procedure. If this happens it is very easy to distinguish them in the same way in which SSA is applied to distinguish healthy from unhealthy mechanical structures [31].

2 Method

2.1 Experimental rig

Experiment was carried out on a single stage centrifugal blower DP1.12 [32]. The inlet pipe had diameter $D_{in} = 300$ mm and was followed by the Witoszynski nozzle and the impeller with 23 blades, vaneless diffuser and circular volute. The rotor inlet diameter at the hub and the inlet span equaled $D_{1hub} = 86.3$mm and $b_1 = 38.9$ mm, respectively. At the outlet those values changed to $D_2 = 330$ mm and $b_2 = 14.5$ mm. The diffuser outlet diameter was equal to $D_3 = 476$ mm. The volute radius was gradually increasing streamwise from the volute tongue gap of 5 mm towards the outlet pipe of diameter $D_{out} = 150$ mm. A throttling valve was mounted at the end of the outlet pipe. The rotor was driven by an asynchronous alternating current (AC) motor with the rotational speed of 100 Hz that corresponded to a flow rate of 0.75 kg/s and pressure ratio PR = 1.08. Rotational speed yielded the impeller tip speed equal to 103 m/s.

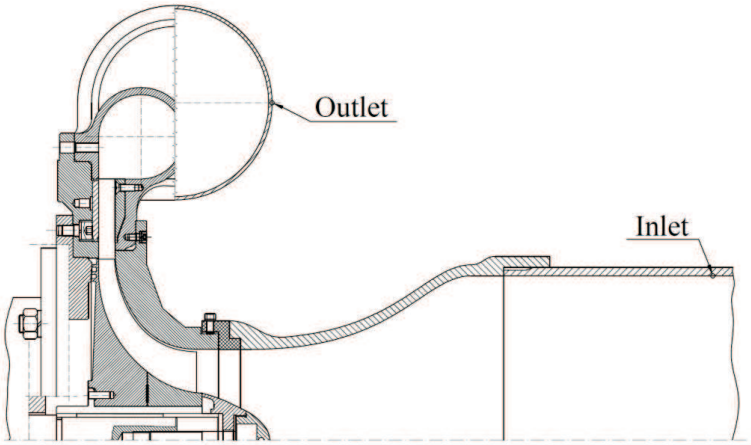

Figure 3: Cross section of the experimental rig used in this study with positions of the pressure gauges.

The test stand was equipped with 2 dynamic subminiature Kulite transducers (XCQ-093-5D, natural frequency 150 kHz) connected to an Iotech Wavebook 516/E data acquisition system. Their position is presented on the stand cross-section in Fig. 3. Transducers were mounted flush to the walls to measure the static pressure at the rotor inlet and at the volute outlet. Similarly to previous studies performed on this stand the position of the throttling valve was described by the dimensionless throttle opening area parameter referred to as TOA.

$TOA = 100\%$ corresponds to fully opened valve, while $TOA = 0\%$ corresponds to fully closed valve. Each signal contained 2^{21} samples gathered with the frequency of 100 kHz. The temperature was controlled and remained constant during the entire experiment at 26 °C.

2.2 Singular spectrum analysis approach

The methodology used here is based on PCA which is a statistical procedure that uses an orthogonal transformation to convert a set of multivariate observations into a set of linearly correlated variables. However, PCA generally assumes that the data components are independent, but in the case of time series, the values are generally nonindependent, and thus an extension of PCA called singular spectrum analysis (SSA) provides a better alternative [27]. SSA is PCA applied to lag versions of a single time series variable. It follows the following four steps:

Data collection: The variables measured, in this particular case the pressure, are arrange in vectors with length N as $\mathbf{x} = (x_1,\ x_2,\ \ldots x_j, \ldots,\ x_N)$ where $j = 1, 2, \ldots,\ N$.

Embedding: Given a window with the time series by W points ($1 < W \leq \frac{N}{2}$) the W – time lagged vectors arranged in columns are used to define the trajectory matrix $\widetilde{\mathbf{X}}$. These vectors are padded with zeros to keep the same vector length.

$$\widetilde{\mathbf{X}} = \begin{pmatrix} x_1 & x_2 & x_3 & \ldots & x_w & \ldots & x_W \\ x_2 & x_3 & x_4 & \ldots & x_{w+1} & \ldots & x_{W+1} \\ x_3 & x_4 & x_5 & \ldots & x_{w+2} & \ldots & x_{W+2} \\ x_4 & x_5 & x_6 & \ldots & x_{w+3} & \ldots & \vdots \\ x_5 & x_6 & \vdots & \ldots & \vdots & \ldots & x_N \\ x_6 & \vdots & \vdots & \ldots & x_N & \ldots & 0 \\ \vdots & \vdots & x_N & \ldots & 0 & \ldots & 0 \\ \vdots & x_N & 0 & \ldots & 0 & \ldots & 0 \\ x_N & 0 & 0 & \ldots & 0 & \ldots & 0 \end{pmatrix} \tag{1}$$

The embedding matrix $\widetilde{\mathbf{X}}$ is the representation of the system in a succession of overlapping vectors of the time series by W-points.

Decomposition: The empirical orthogonal functions (EOFs), which represent the principal directions of the system, are calculated by the eigenvalue and eigenvector decomposition of $\mathbf{C}_X = \frac{\widetilde{\mathbf{X}}'\widetilde{\mathbf{X}}}{N}$ (where $\widetilde{\mathbf{X}}'$ denotes the transpose matrix of $\widetilde{\mathbf{X}}$) by solving the eigenvalue problem defined

$$\mathbf{C}_X \rho_k = \lambda_k \rho_k \quad . \tag{2}$$

The decomposition into eigenvalues yields k-eigenvalues and k – eigenvectors which define orthonormal basis of the decomposition of $\widetilde{\mathbf{X}}$. The eigenvalues λ_k are ordered in decreasing and the eigenvectors ρ_k in the same order that their corresponding eigenvalues. Each eigenvalue defines the partial variance in the direction of its corresponding eigenvector, therefore the sum of all eigenvalues gives the total variance of $\mathbf{X}$.

The decomposition into a certain number of principal components (PCs) of the source signal provides the distribution of the autocorrelated variance among these components. Projecting the measured data $\widetilde{\mathbf{X}}$ onto the EOFs matrix yields the corresponding PC matrix $\mathbf{A}$ which contains the variance information distributed among these PCs:

$$A_n^k = \sum_{w=1}^{W} x_{n+w-1} \rho_n^k \quad . \tag{3}$$

Reconstruction: A certain number of reconstructive components (RCs) are reconstructed by using the part of a time series that is associated with a single EOF or several by combining the associated PCs

$$R_n^k = \frac{1}{W} \sum_{w=1}^{W} A_{n-w+1}^k \rho_n^k \, , \tag{4}$$

where k – eigenvectors give the k^{th} RC at n – time between $n = 1, \ldots, N$ which was embedded in a w – lagged vectors with the maximum W – length.

The variance is distributed into the RCs in a decreasing order from the first components until the last ones. Therefore, the first RCs contain much more descriptive information of the dynamical system than next ones. By the use of a certain number of RCs, an approximated reconstructed source signal was developed.

2.3 Clusterisation

This section introduces the effect of clusterisation in order to be used as a metric for distinguishing between stable and not stable phenomena. The RCs obtained

in the signal decomposition are used as reference state, which describes an stable working condition of the turbocompressor. The detection whether the system is stable or not stable is based on the comparison of an observation signal to the reference state. A new observation signal is multiplied with the RCs (inner product between two vectors) and hence projected in the reference space constructed by the RCs

$$\mathbf{T} = \mathbf{x}_{\mathrm{s}}\mathbf{R}\ , \tag{5}$$

where $\mathbf{T}$ is the transformation of the observation signal $\mathbf{x}_{\mathrm{s}}$ onto the reference space $\mathbf{R}$. The dimension of the reference space is $p \leq W$. Therefore, when two observation signals are compared onto the reference space, it is expected that if the two observation signals are similar, the distance between them is minimum, however if they are different, the distance between them will increase.

3 Results

3.1 Regions of operation of the machine

Figures 4 and 5 present pressure values as a function of the throttle opening area obtained based on the outlet and inlet signals respectively. Grey area represents the region between minimal and maximal values obtained in each valve position throughout the measurement. Bold line connects average values registered therein. Each of 146 measurements presented in the plot contained 2^{21} samples gathered with the frequency of 100 kHz. This means that measurement lasted over 20 s and corresponded to over 2000 impeller rotations. A similar phenomenon to the represented in these plots was observed in all the measurements during the experiment.

3.2 Base constructed from first two reconstructed components (RC1 and RC2)

Figures 6 and 7 represent families of signals gathered at $TOA < 65\%$. All of them are projected into two-dimensional space constructed in a way described in Sec. 2.3. This space is spanned by two principal components named as RC1 and RC2 henceforth. These are two initial components obtained in the SSA method conducted on signal gathered in the blower nominal point ($TOA = 30\%$). The value of throttle of each projected signal is marked with an adequate color corresponding to a colorbar.

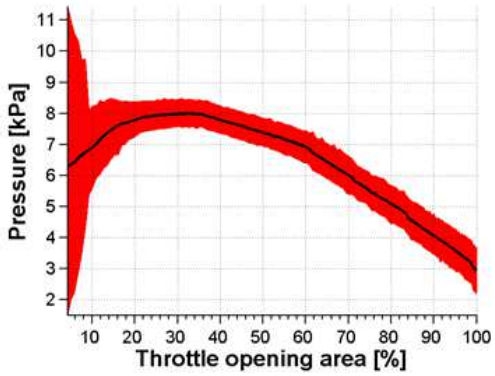

Figure 4: Blower outlet min-to-max and average pressure in a function of the throttle opening Area (Copyright ©2014 Elsevier).

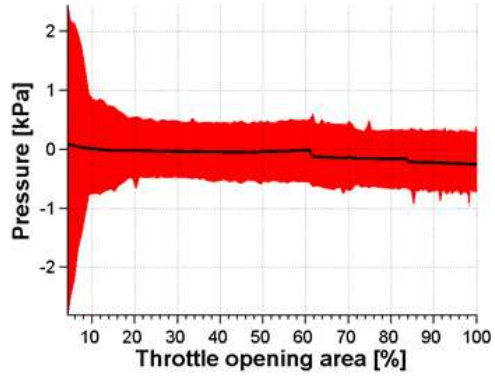

Figure 5: Blower inlet min-to-max and average pressure in a function of the throttle opening area (Copyright ©2014 Elsevier).

4 Discussion

4.1 Three flow conditions

Based on Figs. 4 and 5 one can distinguish 3 phases of operation of the machine in analyzed control points. At $TOA > 20\%$ it was working in a stable manner with constant min-to-max span caused by a local pressure fluctuations and inevitable signal noise. The average pressure in inlet was close to zero at all circumstances. The average outlet pressure was rising and dropping by following the blower performance curve. At $9\% < TOA < 20\%$ the amplitude of pressure oscillation

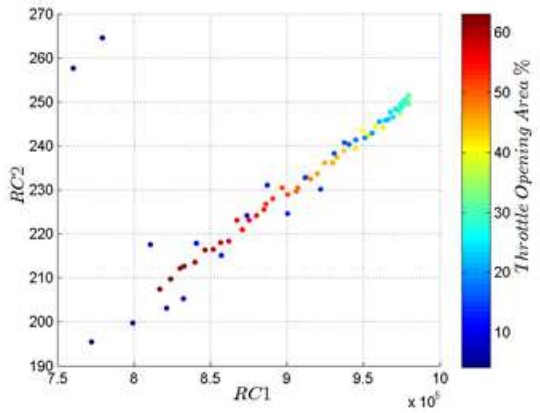

Figure 6: Points representing outlet pressure signals in a space constructed from the principal base (RC1, RC2) used in this study.

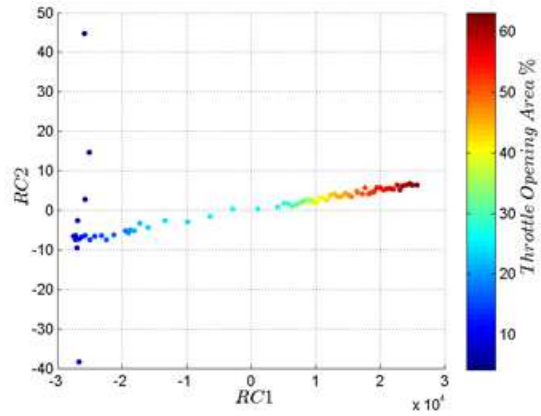

Figure 7: Points representing inlet pressure signals in a space constructed from principal base RC1, RC2 used in this study.

significantly raised in both locations indicating appearance of flow instability. It can be, however, regarded as moderate as the amplitude rise was not bigger than twice in size. Nevertheless, the observed phenomenon can be regarded as global for the machine, as it was observed in both control points. According to widely

accepted nomenclature [3,4,7,32,33] this state can be regarded as mild surge or transient phase before inception of the deep surge. At $TOA < 9\%$ the amplitude of oscillations rose significantly. In inlet it equaled 5 kPa, while in the outlet around 10 kPa. This difference clearly corresponds to a Greitzer model, where oscillations are strongest in the plenum [6,7] and hence, the surge was observed.

4.2 Representation of the signals in reference space RC1, RC2

Based on Figs 6 and 7, one can distinguish the different working conditions of the machine operation phases. The observation signals are projected onto the reference space which is able to identify alterations within the dynamical system [28,34,35]. In both plots points representing pressure signal have a tendency to be projected along a straight line.

Figure 6 represents the projection of the observation signals onto the reference state created by the signals measured in the outlet. Results suggest that this analysis can be also used to identify the nominal working conditions of the machine similarly to a correlation integral applied by Gu *et. al* [34]. All points are aligned until the machine goes to deep surge condition ($TOA < 10\%$). In this case, the points move away from the straight line, which indicates the unstable phenomena. It can be also observed that the optimum working conditions are around at $TOA = 30\%$ where all points concentrates in a cloud of point. This indicates that the system nominal working conditions are attained at this TOA.

Figure 7 represents the projection of the observation signals onto the reference state of signal measured in the inlet. It can be observed that for observations corresponding to $30\% > TOA > 20\%$ the spacing between points increases and hence it alerts that deep surge is about to occurs. This is very important, that the indication appears so quickly, because this measurement point is located further upstream of the impeller compared to studies, where the inlet recirculation was normally observed [32,36,37]. This phenomenon is known to strongly influence the variations of the signal in the phase space, and hence would be strongly influencing position of the points in given projection [31]. Nevertheless, it could be observed, that even in other control points analysis of pressure signal could give indication of incoming surge inception. However in this range, the points are still proportionally aligned by the contribution of RC1 and RC2. When the $TOA < 10\%$, the machine enters deep surge condition (global effect). This phenomena could be clearly distinguished because their projection points move away from the line and the spacing becomes enormous. This gives again very clear indication between stable and unstable signals.

5 Summary

In presented study the signals were gathered in inlet and outlet zones of the centrifugal blower and subject to dynamical study by means of the singular spectrum analysis. Signal was decomposed into a principal components that were used to reconstruct the reference space by means of the reconstructive components. The projection of the observation signals onto the reference state was studying in order to identify different working conditions of the centrifugal blower. The analysis was implemented in signals measured in the inlet and outlet by different throttle opening areas that defines different working conditions. The main conclusions of this study are listed below:

- Method allows to distinguish between stable and unstable working conditions by considering points spacing and positioning in relation to another points. The results obtained clearly align with the results obtained in a previous study by the authors [31]. However this analysis is able to characterise dynamical responses in multidimensional vectors that make easier the visualization of the surge effect.
- The projection of the signals onto the reference state provides information of global effects such as deep surge but also local effects.
- Apart from detecting unstable flows method could be also applied for specifying nominal working conditions of the blower.
- The use of two dimensions of the reference space (RC1 and RC2) is enough to detect the phenomena described by different working conditions at different TOA.

Received in July 2016

References

[1] Emmons H.W., Pearson C.E., Grant H.P.: *Compressor surge and stall propagation*. Trans. ASME **77**(1955), 4, 455–469.

[2] Bousquet Y. *et al.*: *Analysis of the unsteady flow field in a centrifugal compressor from peak efficiency to near stall with full-annulus simulations*. Int. J. Rotat. Mach. (2014), ID 729629, DOI:10.1155/2014/729629.

[3] Greitzer E.M.: *Surge and rotating stall in axial flow compressors – Part I: Theoretical compression system model*. J. Eng. Gas Turb. Power **98**(1976), 2, 190–198.

[4] Greitzer E.M.: *Surge and rotating stall in axial flow compressors – Part II: Experimental results and comparison with theory*. J. Eng. Gas Turb. Power **98**(1976), 2, 199–211.

[5] Hansen K.E, Jorgensen P. and Larsen P.S.: *Experimental and theoretical study of surge in a small centrifugal compressor*. J. Fluids Eng. **103**(1981), 3, 391–395.

[6] Elder R.L., Gill M.E.: *A discussion of the factors affecting surge in centrifugal compressors*. ASME J. Eng. Gas Turb. Power **107**(1985), 499–506.

[7] Fink D.A., Cumpsty N.A., Greitzer E.M.: *Surge dynamics in a free-spool centrifugal compressor system*. J. Turbomach. **114**(1992), 2, 321–332.

[8] Gravdahl J.T., Egeland O.: *Compressor surge control using a close-coupled valve and backstepping*. American Control Conf., Proc. 1997, Vol. 2. IEEE, 1997.

[9] Willems F. *et al. Positive feedback stabilization of centrifugal compressor surge*. Automatica **38**(2002), 2, 311–318.

[10] Meuleman C.: *Measurement and unsteady flow modelling of centrifugal compressor surge*. PhD thesis, Technische Universität Eindhoven, 2002.

[11] Van Helvoirt J., De Jager B.: *Dynamic model including piping acoustics of a centrifugal compression system*. J. Sound Vib. **302**(2007), 1, 361–378.

[12] Yoon S.Y. *et al.*: *An enhanced greitzer compressor model including pipeline dynamics and surge*. J. Vib. Acoust. **133**(2011), 5, 51–55.

[13] Macdougal I., Elder R.L.: *Simulation of centrifugal compressor transient performance for process plant applications*. J. Eng. Gas Turb. Power **105**(1983), 4, 885–890.

[14] Botros K.K.: *Transient phenomena in compressor stations during surge*. J. Eng. Gas Turb. Power **116**(1994), 1, 133–142.

[15] Frigne P., Van den Braembussche R.: *Distinction between different types of impeller and diffuser rotating stall in a centrifugal compressor with vaneless diffuser*. J. Eng. Gas Turb. Power **106**(1984), 2, 468–474.

[16] Levy Y., Pismenny J.: *The number and speed of stall cells during rotating stall*. In: Proc. Turbo Expo, Atlanta 2003.

[17] Harley P., Spence S., Filsinger D., Dietrich M., Early J.: *Meanline modeling of inlet recirculation in automotive turbocharger centrifugal compressors*. J. Turbomach. **137**(2015), 1, 11–17.

[18] Botros K., Henderson J.: *Developments in centrifugal compressor surge control — A technology assessment*. J. Turbomach. **116**(1994), 2, 240–249.

[19] Pinsley J.E. *et al.*: *Active stabilization of centrifugal compressor surge*. J. Turbomach. **113**(1991), 4, 723–732.

[20] Nakagawa K. *et al.*: *Experimental and Numerical Analysis of Active Suppression of Centrifugal Compressor Surge by Suction-Side Valve Control*. JSME Int. J. Ser. B. **37**(1994), 4, 878–885.

[21] DiLiberti J.L. *et al.*: *Active control of surge in centrifugal compressors with inlet pipe resonance*. ASME paper 96-WA/PID-1, 1996.

[22] Hafaifa A., Ferhat L., Kouider L.: *A numerical structural approach to surge detection and isolation in compression systems using fuzzy logic controller*. Int. J. Control, Autom. Syst. **9**(2011), 1, 69–79.

[23] Williams J.E., Huang X.Y.: *Active stabilization of compressor surge*. J. Fluid Mech. **204**(1989), 245–262.

[24] Haugen R.L., Meng J.K.: *Method for detecting the occurrence of surge in a centrifugal compressor by detecting the change in the mass flow rate*. United States patent 6, 213, 724. 2001 Apr. 10.

[25] McKee R.J., Carl E.E.: *Method and apparatus for detectingt the occurrence of surge in a centrifugal compressor*. United States patent US 6, 981, 838. 2006 Jan. 3.

[26] Jolliffe I.: *Principal Component Analysis*, Vol. 487. Springer-Verlag, New York 1986.

[27] Golyandina N., Nekrutkin V., Zhigljavsky A.: *Analysis of Time Series Structure: SSA and Related Techniques*. CRC Press, 2001.

[28] Garcia D., Trendafilova I.: *A multivariate data analysis approach towards vibration analysis and vibration-based damage assessment. Application for delamination detection in a composite beam*. J. Sound Vib. **333**(2014), 25, 7036–7050.

[29] Jungowski W.M., Weiss M.H., Price G.R.: *Pressure oscillations occurring in a centrifugal compressor system with and without passive and active surge control*. J. Turbomach. **118**(1996), 1, 29–40.

[30] Gysling D.L. *et al.*: *Dynamic control of centrifugal compressor surge using tailored structures*. J. Turbomach. **113**(1991), 4, 710–722.

[31] Garcia D., Stickland M., Liśkiewicz G.: *Dynamical system analysis of unstable flow phenomena in centrifugal blower*. Open Eng. **5**(2015), 1, 332–342.

[32] Liśkiewicz G. *et al.*: *Identification of phenomena preceding blower surge by means of pressure spectral maps*. Exp. Therm. Fluid Sci. **54**(2014), 267–278.

[33] de Jager B.: *Rotating stall and surge control: A survey*. In: Proc. 34th Conf. on Decision and Control. IEEE, 1995.

[34] Gu C. *et al.*: *Observation of centrifugal compressor stall and surge in phase portraits of pressure time traces at impeller and diffuser wall*. J. Fluids Eng. **129**(2007), 6, 773–779.

[35] Komatsubara Y., Mizuki S.: *Dynamical system analysis of unsteady phenomena in centrifugal compressor*. Int. J. Therm. Sci. **6**(1997), 1, 14–20.

[36] Mizuki S., Oosawa Y.: *Unsteady flow within centrifugal compressor channels under rotating stall and surge*. J. Turbomach. **114**(1992), 2, 312–320.

[37] Tamaki H.: *Experimental study on surge inception in a centrifugal compressor*. Int. J. Fluid Mach., Syst. **2**(2009), 4, 409–417.